NASA

Technical Memorandum **82022**

Voyager Measurement of the Rotation Period of Saturn's Magnetic Field

M. D. Desch
M. L. Kaiser

JANUARY 1981

National Aeronautics and Space Administration

Goddard Space Flight Center
Greenbelt, Maryland 20771

VOYAGER MEASUREMENT OF THE ROTATION PERIOD OF SATURN'S MAGNETIC FIELD

M. D. Desch and M. L. Kaiser

NASA/Goddard Space Flight Center
Laboratory for Extraterrestrial Physics
Planetary Magnetospheres Branch
Greenbelt, Maryland 20771

to appear in Geophys. Res. Lett.

Abstract. We determine Saturn's radio rotation period using measurements made by the Planetary Radio Astronomy experiment onboard the Voyager spacecraft. The sidereal period deduced, 10 hr 39 min 24 sec ± 7 sec, is within the 10 hr to 11 hr range of optical periods derived from a century of atmospheric spot and Doppler spectroscopy observations. The radio rotation period is presumably that of the planet's magnetic field. We propose a provisional Saturn longitude convention, and we provide equations to compute a longitude ephemeris and to transform between the proposed system and the (10 hr 14 min) system used for the Pioneer 11/Saturn encounter. In addition, we evaluate the degree of longitude smearing which could result over the long term from the merging of data sets organized in this system. Finally, no evidence of control of the radio emission by any of Saturn's satellites is found.

Introduction

Using Voyager Planetary Radio Astronomy (PRA) data, Kaiser et al. (1980) recently provided the first conclusive evidence for the emission of nonthermal radio waves from Saturn. From an initial survey of 40 days of data, they observed that the Saturnian kilometric radiation (SKR) is sporadic, strongly and exclusively right-hand polarized, and that it occurs primarily at kilometer wavelengths. They further reported a provisional value for the rotation period of Saturn's magnetic field based on the presence of statistically significant modulation of the radio events and on the assumption of planetary magnetic field control over the event occurrence statistics. The period they reported, 10 hr 39 min 54 sec (±36 sec), was within the range of optical periods derived from Doppler spectroscopy (Moore, 1939) and from measurements of spots (Hall, 1877; Reese, 1971). In the present paper we extend and improve upon the rotation period analysis of Kaiser et al. in two important ways. First, by extending the analysis interval by a factor of about 7, to 267 days, we are able to determine the absolute sidereal rotation period to within ±7 sec. And, second, we propose adoption of a longitude system adequate to the needs of Voyager and Pioneer 11 investigators who wish to organize their data in a consistent fashion at Saturn's intrinsic rotation

rate. We provide an equation which generates this longitude system. In addition, an equation is provided permitting translation between the right-handed (10 hr 14 min) system used by the Pioneer 11 investigators during the September, 1979 Saturn encounter and the left-handed (10 hr 39 min 24 sec) system derived here.

Observations

The present study makes use of Voyager PRA data extending from the date of first detection of SKR, January 1, 1980, through September 23, 1980, a 267-day interval corresponding to 600 rotations of Saturn. During this period we observed 520 SKR events totaling 300 hr of activity. (For the purpose of this report we define an event as the continuous detection of SKR, lasting anywhere from several minutes to several hours.) Taking into account the total duration of interference-free monitoring, this corresponds to an average occurrence probability of 7%, or an average of almost 0.9 events (or 30 min of activity) per rotation. This occurrence rate was by no means uniform over the analysis interval, however, reflecting the fact that Voyager 1 (V1) was approaching the planet, thus increasing the likelihood of detection. For example, the average occurrence probability was only 3% during the first half of the analysis interval but 12% during the second half.

We have continued to use the methods described by Kaiser et al. (1980) in identifying SKR in PRA frequency-time spectrograms. Briefly, where simultaneous coverage existed, identifications were confirmed through comparison of Voyager 2 (V2) records with those from V1. That is, SKR was identified by virtue of its greater intensity and earlier occurrence in the V1 records owing to the proximity of V1 to Saturn. Where dual spacecraft coverage did not exist, identifications were based on the polarization and dynamic spectral appearance alone. However, fewer than 15% of the events were identified in this way. Although V2 data were used in this corroborative fashion, V1 data were used exclusively in forming the time series from which the rotation period was derived because the V1 data constituted by far the larger of the two data sets.

A sample record of multiple SKR events on August 14, 1980 is shown in Fig. 1. By this point in time, SKR clearly dominates PRA dynamic spectra observed by V1. The Jovian emission, appearing primarily in the high-frequency

(bottom) half of the spectrum at 0300-0330 spacecraft event time (SCET), is noticably weaker than the SKR. Unusually strong and well-defined frequency drifting SKR events can be seen from 0230-0330 and from 1230-1400 SCET centered at about 250 and 400 kHz, respectively. In addition, a broad region of amorphous SKR is seen from 0400-0900 and from 1630-1730 SCET over the same frequency band.

Procedure

We summarize in this section the steps used to derive Saturn's rotation period and calculate an associated uncertainty. As observed by Voyager 1, all events were recorded in spacecraft event time in a frame which is moving relative to Saturn. In order to compute the rotation period in the desired sidereal frame, the start and stop time of each event was corrected for light travel time between Saturn and V1. Over the duration of the analysis interval (267 days) the magnitude of the light time correction varied from 23.3 to 3.8 min. Correction for the motion of the spacecraft in azimuth relative to Saturn's ascending node (motion in right ascension) was not considered necessary since the SKR beam is believed to be fixed relative to the Saturn-sun line rather than rotating with the planet (Warwick et al., 1981). In any event, adjustment of the event times for right ascension motion leads to a change in the sidereal period which is much less than the uncertainty in the period.

Following adjustment of the start and stop times for light-travel time, the PRA data were represented by a time series consisting entirely of 1's and 0's. The 1's correspond to the times of SKR emission and the 0's to times when observations were made but no SKR was recorded. The time series was analyzed using a method of power spectral analysis applicable to data, such as ours, which are sampled at irregular intervals (Deeming,1975). A least-squares method was then used to refine the period found by spectral analysis of the time series. The data were linear least-squares fit to an equation of the form $\lambda_i = a + br_i$, where the rotation phase, λ_i, of each event was expressed as a function of its integral rotation number, r_i. Rotation numbering began on Jan 1.0, 1980. As a first step, rotation phase and number were computed using the estimated sidereal period derived from the spectral analysis. Any residual trend in the data, that is, any tendency for the event longitudes to

increase or decrease with time is then indicated by a finite positive or negative value of the the least-squares slope, b. The best estimate of the sidereal rotation period is then obtained through iterative regression until b approaches zero or is within one standard deviation (σ_b) of b.

Finally, an estimate of the uncertainty in the derived period is obtained by performing the regression many times using a range of starting values around that which gives the best fit. Owing to the scatter of the data in rotation phase, some of these analyses will yield first iteration slopes which are statistically insignificant ($b<\sigma_b$), indicating a range of rotation periods which are compatible with the accepted value. The difference between the largest and smallest such rotation period is taken to be the uncertainty in the period. The uncertainty so obtained is larger than that which would be derived from using σ_b alone (the formal error) but it is undoubtedly a more meaningfull estimate.

Results

The result of applying the above procedure up to and including calculation of the power spectrum is shown in Fig. 2. The spectrum is constructed of events which occurred at a single frequency, in this case 174 kHz, and which exceeded a flux density threshold of 10^{-19} W m^{-2} Hz^{-1} normalized to a constant 1 AU distance between the observer and Saturn. Events above this particular threshold were easily detected over the entire analysis interval. The lower panel shows a low-resolution survey extending over a wide spectral window from periods of 10 hr to 1000 hr. The upper panel shows a high-resolution spectrum, of the same data, centered approximately on the principal peak in the survey spectrum. The average time resolution of this spectrum is near the practical limit of about 65 sec. Both are plotted in terms of the standard deviation (σ) of the spectral power above the 'noise' level inherent in each spectrum.

The survey spectrum (bottom panel) spans the revolution periods of all of Saturn's major satellites and the expected period, as viewed from Saturn, of persistent solar wind features such as interplanetary magnetic field reversals. In greater detail, the high resolution spectrum (top panel) spans the $\sim$ 10 hr to $\sim$ 11 hr range of periods of Saturn's surface features and clouds (Moore, 1939; Reese, 1971). Examination of the survey spectrum

indicates only one significant peak, near 10 hr, which is shown by the high-resolution spectrum to occur at ~ 10.66 hr. This feature is a factor of 5 above the second strongest peak (near 260 hr) in the spectrum and approximately 16σ above the survey spectrum noise level. We attribute this spectral feature to the modulation of the SKR by Saturn's rotation. With regard to possible satellite modulations, we find no evidence of spectral power at the appropriate satellite periods or their heterodynes with the rotation period. In fact, none of the secondary peaks exceed 4σ above the survey spectrum noise level and, further, their power levels have declined steadily with the accumulation of data. Thus at this stage of the analysis we have found no Saturn analog of the well-known phenomenon whereby some of Jupiter's sporadic radio emission is controlled by Io. There is also no indication of spectral power at the low-frequency end of the survey spectrum where longer-term modulations such as those due to solar influences might appear. However, far too few cycles of such long-term modulations are included in the time series to yield a definitive test. For example, only about 10 cycles of a 26-day solar periodicity could have occurred over the analysis interval. Finally, although not shown, no significant spectral power was found at periods <10 hr except at the harmonics of the rotation period.

Looking at the high-resolution spectrum, we note the 5σ spike on the low-frequency shoulder of the SKR spectral peak. This spike occurs at a period of about 10.69 hr and appears to be due to a low intensity component of the SKR which reappears at a different, slightly longer period than that of the principal source. This component is not expected to significantly bias the principal spectral peak because it lies well outside the 65-sec half-power spectral bandwidth of the peak. This component of drifting SKR is discussed again below where it appears explicitly in Fig. 3.

We have refined this power spectrum determination of the period according to the linear least-squares method described previously and illustrated now in Fig. 3. Here the SKR events are indicated by vertical bars plotted as a function of longitude and rotation number. (Longitude is defined arbitrarily in this figure in order to place most of the the events near 180° for clarity.) As in Fig. 2 we have plotted only events at 174 kHz which exceeded 10^{-19} W m^{-2} Hz^{-1}. It is evident that one range of longitudes is favored, namely that from about 100 to 270 degrees; this is particularly apparent in the occurrence probability histogram plotted on the right of Fig. 3. Fig. 3

(bottom) actually illustrates the final organization of the data in rotation phase following several least-squares iterations. That is, events were first organized in rotation phase and rotation number using the provisional power spectrum period (10.66 hr). This yielded a small but statistically significant negative value for the least-squares coefficient, b (the slope), thus indicating a general trend in the event longitudes toward decreasing values with time. Clearly the optimum period is that one which removes any linear drift in the event longitudes. This period was found through successive iteration to yield the results shown in the Fig. 3. Using a sidereal rotation period of 10 hr 39 min 24 sec (corresponding to a rotation rate of 810.76 deg/day), the least-squares fit, shown via the dashed line, gave zero slope within $\pm \sigma_b$. Least-squares analysis using initial starting periods ranging from 10.6545 through 10.6585 hr yielded statistically insignificant trends in longitude from which, as described in the previous section, we derive an uncertainty of $\pm(10.6585-10.6545)/2$, or ± 7 sec, in the measured period.

Along the top of Fig. 3 is shown the time history of the rotation period as a function of the end point of the analysis interval. Rotation periods were computed in 30-rotation increments with each successive computation including all of the preceding data. Because the individual determinations are not independent they give a deceptively good impression as to the magnitude of the scatter with time; however, the figure does show how the measurements are converging with the accumulation of data.

It is probably apparent from the dashed-line intercept in the figure that in performing the least-squares computation only the events within the main peak were used, that is, those events which occurred between 100 and 270 degrees longitude. This had the effect of eliminating 27% of the data from the final step of the analysis. The reason for this restriction is that we wished to confine the analysis to those events which presumably resulted from successive passages of one and the same emission cone past the spacecraft. In other words, rather than allow the least-squares determination to be influenced by radio events which may have occurred in association with side or back lobes of the main beam, we restricted attention to the main-beam events alone. Although the problem is conceptually simpler when expressed and performed in this way, it has the disadvantage of requiring somewhat subjective decisions regarding the choice of main-peak longitude boundaries.

Thus, in order to assure the precision of the period determination, we have tested the sensitivity of the technique to a broad range of possible variations in methodology, including the use of a range of longitude boundaries, the use of intensity weighted as opposed to unweighted regressions, the exclusive use of event start times instead of both start and stop times, and the use of events at numerous other frequencies in the SKR band. Except for an analysis at 385 kHz which differed from the proposed period by 1.6 σ_b, none of the variations yielded a rotation period which differed by more than 0.7 σ_b from that quoted. Further, we have subjected the entire analysis procedure to an independent test by measuring Jupiter's sidereal rotation period. Because Jupiter's period is a known quantity, this constitutes a test of the accuracy of the procedure. We used Planetary Radio Astronomy detections of Jupiter near 1 MHz made from Voyager 1 over the period 1977 November to 1978 June (Kaiser et al., 1979), approximately equivalent to the Saturn data set both in terms of the extent of the analysis interval and the total number of events. Using the identical procedure followed for Saturn, except of course for the light time and right ascension corrections which applied to the Voyager-Jupiter instead of the Voyager-Saturn geometry, we derived a rotation period of 9 hr 55 min 29.6 sec $\pm$ 1.1 sec, or only 0.1 sec less than the accepted period (Riddle and Warwick, 1976). The $\pm$1.1 sec uncertainty is smaller in this case than that quoted above for Saturn because, as noted by Kaiser et al. (1980), the Jovian emission is more highly organized in rotation longitude than is SKR.

We noted with regard to Fig. 2 the appearance of statistically significant spectral power at 10.69 hr, corresponding to a second, weak component of SKR. This component is visible in Fig. 3 as those SKR events which are clearly not locked in rotation phase but which 'drift through' the plot from early to late longitudes. Note especially rotation numbers 225 through 300 and 350 through 425. These events are much more conspicuous in plots in which no intensity threshold has been set, implying that they correspond to a weaker SKR component. They are perhaps analogous to the Jovian nKOM emission which Kaiser and Desch (1980) have shown is related to an emission source which fails to rigidly corotate with the Jovian magnetosphere. This component is being investigated further as to other possible distinguishing characteristics.

Longitude Convention

To facilitate consistent use of the rotation period, we propose adoption of the following Saturn longitude system which will be referred to as SLS (Epoch, 1980.0) or, simply, SLS. Like Jupiter's System III, SLS is left-handed (positive west), that is, the longitude increases with time as viewed by a stationary observer. Also like System III, the central meridian is referred to the geometrical rather than to the illuminated disk of the planet so that solar phase angle is irrelevant. The system epoch is 0 hr U.T. on January 1.0, 1980 at which time the prime meridian (0° SLS) is defined to be coincident with Saturn's vernal equinox, or the ascending node of Saturn's orbit on its equator (Sturms, 1971). (We have chosen a system epoch of 1980.0, rather than the more conventional 1950.0, so as to minimize any longitude shift resulting from future updates to the rotation period. Note that a change in the period of as little as 7 sec (the present uncertainty) would introduce a longitude shift of over 1600° over the 30-yr span between 1950 and 1980.) No correction is necessary for equinox precession, owing to its negligible magnitude relative to the present (and anticipated) uncertainty in the measured rotation period. For the same reason the small difference between U.T. and ephemeris time is entirely negligible.

Longitude computation is as follows. If t is the time of any given observation, t_o the system epoch defined above, D the observer-Saturn distance in km, and R the observer right ascension (angle in degrees in Saturn's equatorial plane) from Saturn's vernal equinox to the observer, then the longitude, λ_{SLS}, of the meridian containing the observer is given by

$$\lambda_{SLS} = 810.76\ (t-t_o - 3.86\times10^{-11}\ D) - R, \qquad (1)$$

where the longitude is that facing the observer at the time the light signal left the planet (the central meridian longitude). Note that because the rotation rate constant, 810.76, is in degrees/day, $t-t_o$ must be expressed in days and fractions thereof.

The system proposed here is directed principally at the use of Voyager data; however, for those who wish to order Pioneer 11/Saturn encounter data in the present system, we provide the following transformation equation which is expressed in terms of the sub-Pioneer longitudes based on the 10 hr 14 min rotation period. The relationship is

$$\lambda_{SLS} = 74.6 - \lambda_p - 1.397\ \Delta t, \qquad (2)$$

where λ_{SLS} is the SLS (1980.0) sub-Pioneer 11 longitude, λ_p is the sub-Pioneer 11 longitude using the 10 hr 14 min rotation period (Sturms, 1971), and Δt is the elapsed time in <u>hours</u> from 12.0 hr spacecraft event time on 31 August 1979. Note that the 10 hr 14 min system adopted for the Pioneer/Saturn encounter is a right-hand system, that is, the longitude decreases with time.

Longitude Smearing

Unlike the Jovian case in which the period is known to within an accuracy of at least 0.02 sec, the 7-sec uncertainty in Saturn's period may yield measurable smearing, or 'smoothing', of data organized in rotation phase if the data are collected over a significant span of time. The amount of smearing is straightforward to evaluate, and we do so here in the context of the Voyager-Saturn encounters since a principal use of this period and longitude system will be by Voyager-spacecraft investigators. Propagation of the ± 7 sec uncertainty in the period between the system epoch on Jan. 1.0, 1980 and the Voyager 2 encounter with Saturn on Aug. 27, 1981 yields no more than 91° of rotation phase (longitude) error. Between the Voyager 1 and 2 encounters with Saturn (Voyager 1 encounter is on Nov. 12, 1980), 40° of rotation error can accumulate. And, over the approximate 6-day bow shock-to-bow shock durations of the encounter periods themselves, no more than 0.9° of longitude smearing can take place. This is to be compared with the 200° error which would result over the same 6-day interval if the 10 hr 14 min period adopted for the Pioneer 11 encounter with Saturn were used. Finally, propagation of the ± 7 sec uncertainty in SLS from the System epoch back to the Sept. 1, 1979 epoch of the Pioneer11/Saturn encounter yields a maximum error of 18° in calculations of λ_{SLS} using eq. (2).

Summary

A power spectrum and linear regression technique has yielded a value for Saturn's sidereal rotation period of 10 hr 39 min 24 $\pm$ 7 sec. This corresponds to a rotation rate of 810.76 $\pm$ 0.15 deg/day, which we take to be the rotation rate of Saturn's magnetic field. A left-handed (positive west)

Saturn longitude system (SLS, 1980.0) is described in equation form. The convention has its prime meridian (0° SLS) coincident with Saturn's vernal equinox at 0 hr U.T. on Jan. 1, 1980. Aside from the power appearing at Saturn's rotation period and a minor component at a slightly longer period, the wide-window power spectrum is featureless indicating that there is no evidence for modulation of SKR by any of Saturn's satellites.

References

Alexander, J.K., Note on the beaming of Jupiter's decameter-wave radiation and its effect on radio rotation period determinations, Astrophys. J., 195, 227-233, 1975.

Deeming, T.J., Fourier analysis with unequally spaced data, Astrophys. Space Sci., 36, 137-158, 1975.

Hall, A., On the rotation of Saturn, Astron. Nachr., 90, 145-150, 1877.

Kaiser, M.L. and M.D. Desch, Narrow-band Jovian kilometric radiation: A new radio component, Geophys. Res. Lett., 7, 389-392, 1980.

Kaiser, M.L., M.D. Desch, A.C. Riddle, A. Lecacheux, J.B. Pearce, J.K. Alexander, J.W. Warwick, and J.R. Thieman, Voyager spacecraft radio observations of Jupiter: initial cruise results, Geophys. Res. Lett., 6, 507-510, 1979.

Kaiser, M.L., M.D. Desch, J.W. Warwick, and J.B. Pearce, Voyager detection of nonthermal radio emission from Saturn, Science, 209, 1238-1240, 1980.

Moore, J.H., Spectroscopic observations of the rotation of Saturn, Pub. Astron. Soc. Pac., 51, 274-281, 1939.

Reese, E.J., Recent photographic measurements of Saturn, Icarus, 15, 466-479, 1971.

Riddle, A.C., and J.W. Warwick, Redefinition of System III longitude, Icarus, 27, 457-459, 1976.

Sturms, F.M., Jr., Polynomial expressions for planetary equators and orbit elements with respect to the mean 1950.0 coordinate system, NASA/JPL Tech. Rep. 32-1508, 1971.

Warwick, J.W., Radio emission from Jupiter, Ann. Rev. Astron. Astrophys., 2, 1-22, 1964.

Warwick, J.W., J.B. Pearce, D.R. Evans, T.D. Carr, J.J. Schauble, J.K. Alexander, M.L. Kaiser, M.D. Desch, B.M. Pedersen, A. Lecacheux, G. Daigne, A. Boischot, and C.H. Barrow, Planetary Radio Astronomy observations from Voyager 1 near Saturn, submitted to Science, 1981.

Figure Captions

Fig. 1. Voyager 1 frequency-time dynamic spectrum showing Saturn kilometric radiation (SKR), Jovian emission and solar type III bursts. Increasing darkness is proportional to increasing signal strength. The spectrum covers the 24-hr period beginning at 0 hr spacecraft event time (SCET) on August 14, 1980. The SKR frequency extent is from about 80 kHz to almost 750 kHz. At this time V1 was about 0.8 AU from Saturn and about 3.4 AU from Jupiter.

Fig. 2. Low-resolution (bottom) and high-resolution (top) power spectra of SKR time series. Only events at a single frequency (174 kHz) and above a constant flux threshold were used. Each spectrum shows only a single major peak, corresponding to modulation of SKR at Saturn's rotation period.

Fig. 3. A plot (bottom panel) of the same SKR data as in Fig. 2 in terms of an arbitrary longitude system and rotation number. The data are shown after final organization at the adopted sidereal period as indicated by the least-squares fit (dashed line). The figure in the top panel shows how the period has varied with the accumulation of data. A scale relating calendar date to rotation number is shown between the two panels. The longitude histogram on the right shows how the data are organized in rotation phase.

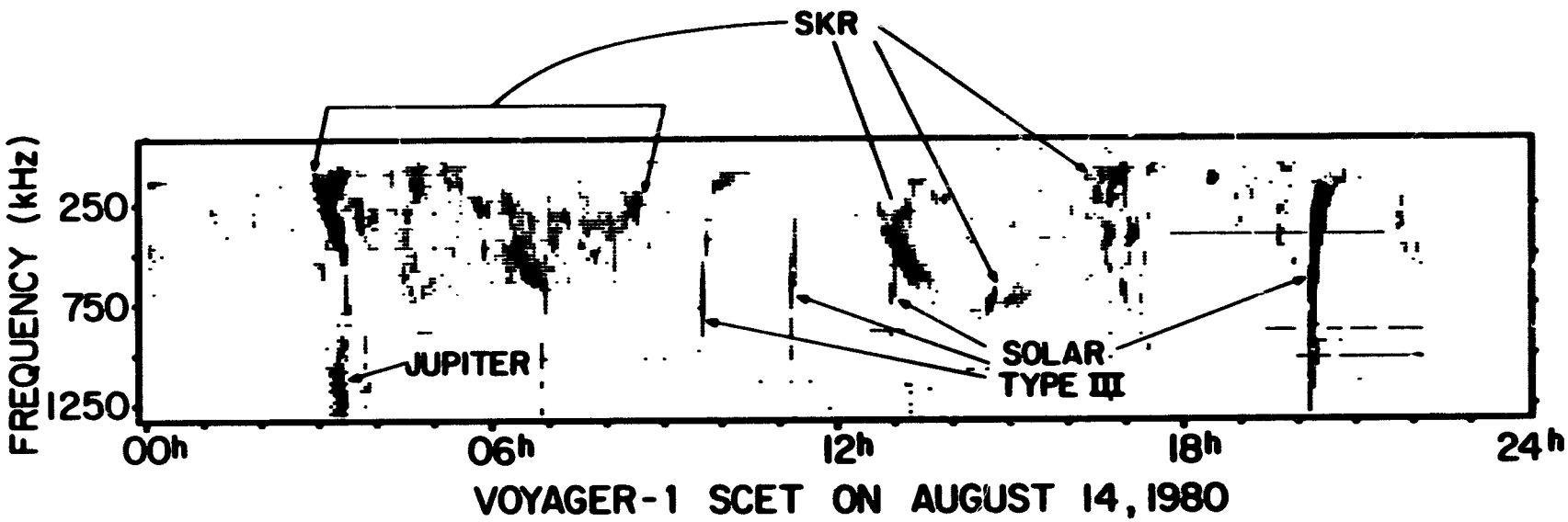
SKR
FREQUENCY (kHz)
250
750
1250
JUPITER
SOLAR
TYPE III
00h
06h
12h
18h
24h
VOYAGER-1 SCET ON AUGUST 14, 1980

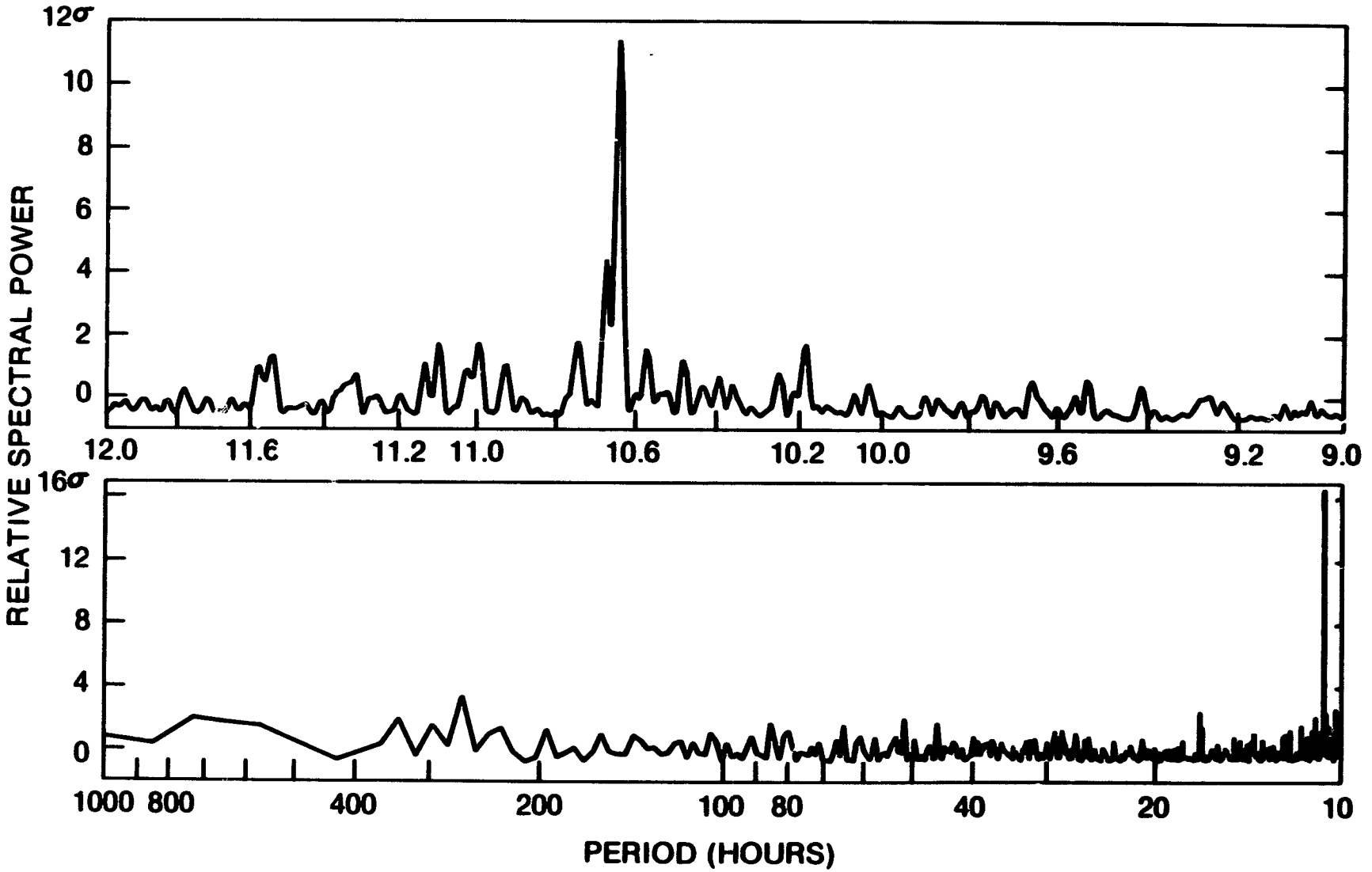
12σ
10
8
6
4
2
0
12.0
11.6
11.2
11.0
10.6
10.2
10.0
9.6
9.2
9.0
16σ
12
8
4
0
1000
800
400
200
100
80
40
20
10
RELATIVE SPECTRAL POWER
PERIOD (HOURS)

Figure 2

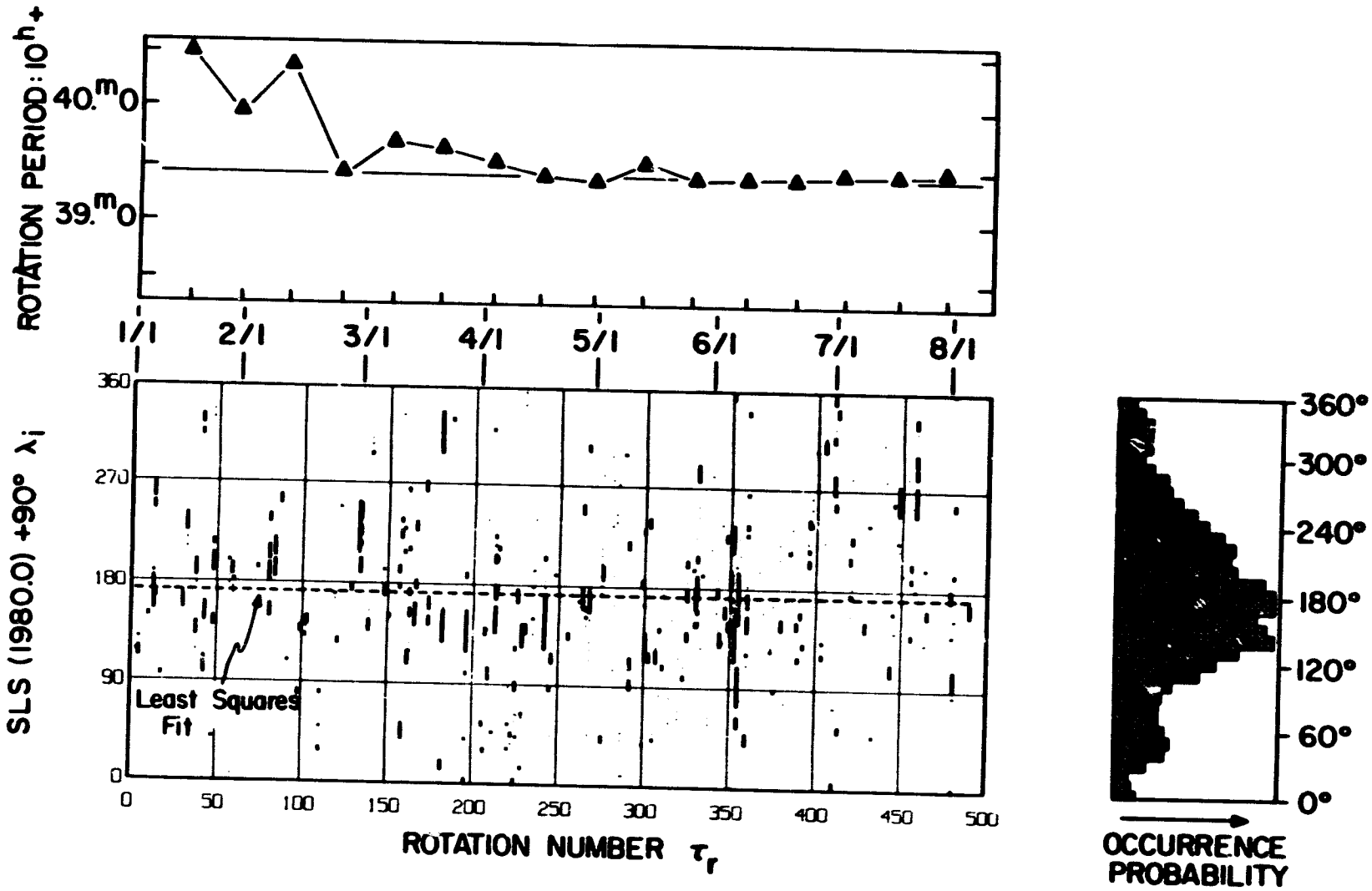
ROTATION PERIOD: 10^h+
40.^m0
39.^m0
1/1
2/1
3/1
4/1
5/1
6/1
7/1
8/1
SLS (1980.0) +90° λi
360
270
180
90
0
Least Squares Fit
0
50
100
150
200
250
300
350
400
450
500
ROTATION NUMBER τr
360°
300°
240°
180°
120°
60°
0°
OCCURRENCE PROBABILITY

Figure 3